LIMNOLOGY and OCEANOGRAPHY

ASLO

Limnol. Oceanogr. 9999, 2024, 1–14

doi: 10.1002/lno.12594

Anoxic waters constrain the vertical distribution of fish developmental stages in an oxygen minimum zone

Juan Gerardo Gutiérrez-Bravo,[1*] **Laura Sánchez-Velasco**,[2*] **Sylvia Patricia Adelheid Jiménez-Rosenberg**,[3] **Mark A. Altabet**,[1] **Sofia Méndez-Mendez**,[4] **Sergio Cambronero-Solano**[5,6]

[1]Department of Estuarine and Ocean Sciences, School for Marine Science and Technology, University of Massachusetts Dartmouth, New Bedford, Massachusetts, USA
[2]Departamento de Oceanología, Instituto Politécnico Nacional-Centro Interdisciplinario de Ciencias Marinas, La Paz, Baja California Sur, Mexico
[3]Departamento de Plancton y Ecología Marina, Instituto Politécnico Nacional-Centro Interdisciplinario de Ciencias Marinas, La Paz, Baja California Sur, Mexico
[4]Unidad de Investigación para el Conocimiento, Uso y Valoración de la Biodiversidad, Centro de Estudios Conservacionistas, Universidad de San Carlos de Guatemala, Ciudad de Guatemala, Guatemala
[5]Departamento de Física, Universidad Nacional de Costa Rica, Heredia, Costa Rica
[6]Department of Research, Colectivo Internacional Pelagos Okeanos, Moravia, San José, Costa Rica

Abstract

In the Eastern Tropical North Pacific Oxygen Minimum Zone (ETNP-OMZ), fish larvae undergo development amidst highly variable dissolved oxygen environments. As OMZs expand, understanding the implications of low-oxygen environments on fish development becomes increasingly relevant for fisheries management and ecosystem modeling. Using horizontal zooplankton tows to track five oxygen levels (oxic [200 μmol/kg], hypoxic [100 μmol/kg] suboxic [10 μmol/kg], anoxic [<1 μmol/kg], and deep [10 μmol/kg at $\sim$ 1000 m depth]), this study analyzed the three-dimensional distribution of fish larvae and adults across the ETNP-OMZ. Results revealed a wide midwater anoxic core, extending from Costa Rica to Baja California, that was almost devoid of fish larvae (< 1 larvae/1000 m^3). Early larval stages primarily inhabited the oxic and hypoxic levels above the core, while postflexion and transformation stages occurred across a wider oxygen gradient, including the deep level below the anoxic core. Epipelagic species (e.g., *Auxis* sp.) were predominantly found in the surface oxic level, whereas coastal-demersal species (e.g., *Bregmaceros bathymaster*, *Ophidion* spp.) were prevalent in the hypoxic level above the core. Meso-bathypelagic species (e.g., *Diogenichthys laternatus*, *Cyclothone* spp.) were present throughout the study area, including below the anoxic core as transformation larvae and juveniles. These findings indicate that a vertical expansion of anoxic waters in OMZs could further constrain the habitat of epipelagic species, while also affecting the ontogenic vertical movements of meso-bathypelagic species.

Oxygen Minimum Zones (OMZs) are typically found at intermediate depths of the open ocean, where dissolved oxygen (DO) concentrations reach low enough values (< 44 μmol/kg) to cause hypoxic stress on marine organisms. In general, OMZs are formed when water mass ventilation is insufficient to resupply DO consumed by aerobic respiration (Karstensen et al. 2007; Stramma et al. 2008; Paulmier and Ruiz-Pino 2009; Tiano et al. 2014). The Eastern Tropical North Pacific Oxygen Minimum Zone (ETNP-OMZ) is the largest and most oxygen-depleted OMZ in the world (Karstensen et al. 2007; Kwiecinski and Babbin 2021). The midwater core of the ETNP-OMZ reaches anoxic conditions (< 1 μmol/kg, below detection limits for common oxygen measuring techniques) in which aerobic respiration is no longer viable (Tiano et al. 2014). This anoxic core is vertically bounded by ventilated warm surface waters above and cold deep-waters below (Margolskee et al. 2019).

*Correspondence: gutijuan@oregonstate.edu; lsvelasc@ipn.mx

Additional Supporting Information may be found in the online version of this article.

Author Contribution Statement: JGGB contributed with formal analyses, methodology, data curation, and writing–original draft preparation. LSV contributed with conceptualization, supervision, and writing–review and editing. SPAJR contributed with methodology, formal analysis, and validation of fish larvae ID. MAA contributed with funding acquisition, supervision, and resources. SMM contributed with onboard methodology and Guatemala permits. SCC contributed with onboard methodology, plotting, and Costa Rica permits.

The upper core boundary is separated from the oxic surface mixed layer by a sharp pycnocline-associated oxycline, where oxygen decreases rapidly over a few tens of meters in depth (Fiedler and Talley 2006; Karstensen et al. 2007). The lower core boundary sees a more gradual change from anoxic (~ 700 m depth), to deep suboxic (1–10 μmol/kg, ~1000 m depth), and hypoxic (10–100 μmol/kg) waters (Fiedler and Talley 2006). These core boundaries serve as habitats for hypoxia-tolerant mesopelagic species that are crucial to the ecosystem function of the ETNP (Wishner et al. 2013, 2018; Sutton et al. 2017).

Increasing deoxygenation due to climate change has been documented in the already oxygen-depleted OMZs (Oschlies et al. 2017; Sánchez-Velasco et al. 2019). Ocean surface warming is causing ocean deoxygenation and expansion of OMZs because not only are gases less soluble in warm waters, but also a warmer, less-dense mixed layer prevents mixing and ventilation of subsurface waters (Oschlies et al. 2018). These factors have caused a decrease in net oxygen concentrations and a shoaling of the upper core boundary (Espinoza-Morriberón et al. 2021). The response of OMZ organisms to this deoxygenation trend is not well-resolved in current climate models (e.g., Archibald et al. 2019; Busecke et al. 2022; Siegel et al. 2023). Small changes from hypoxic to suboxic or anoxic conditions may change ecosystem structure by affecting highly sensitive groups like fish larvae (Sánchez-Velasco et al. 2019). Accordingly, it is necessary to improve the current knowledge of key OMZ ecosystem components.

One poorly understood but economically relevant aspect of OMZ ecosystems is how fish communities are responding to deoxygenation. Because hypoxic stress affects the metabolism and growth of fish, low DO can greatly reduce fish habitat quality (Abdel-Tawwab et al. 2019). For example, in the Eastern Tropical North Atlantic OMZ, billfishes (Xiphiidae and Istiophoridae) and tunas (Scombridae) have contracted their vertical distribution due to shoaling hypoxic waters (Stramma et al. 2012). In the ETNP-OMZ, evidence suggest that expanding hypoxic waters are increasing the habitat of hypoxia-tolerant mesopelagic fish species and reducing the habitat of the epipelagic fish species (Olson et al. 2014; Stewart et al. 2018). These reports suggest that an expansion of low-oxygen waters could detrimentally affect fish populations.

However, comprehensive studies (Gallo and Levin 2016) highlight that OMZ fish assemblages are more tolerant to hypoxia than previously thought. For example, the bristlemouth *Cyclothone* spp., possibly the most abundant vertebrate genus on Earth (Sutton et al. 2010), was abundant at DO concentrations as low as ~ 2 μmol/kg in the lower core boundary of the ETNP-OMZ (Wishner et al. 2013, 2018; Maas et al. 2014). In contrast, a poorly understood aspect of OMZ ichthyofauna is their larval development. The mortality rates in early larval stages impact the recruitment of juveniles into adult populations (Hjort 1914), so a suitable larval habitat is necessary to maintain optimal population sizes (Houde 1987, 2008). The smaller body size of fish larvae reduces the time they can withstand anaerobic respiration (Nilsson and Östlund-Nilsson 2008). Moreover, early larval stages with undeveloped fins (preflexion and flexion larvae) have less effective swimming styles, while later stages with developed caudal and pectoral fins (postflexion and transformation larvae) have greater swimming speeds (Walsh et al. 1989; Moser 1996; Voesenek et al. 2018). For these reasons, early larval stages may be ill-suited to inhabit the hypoxic environments around the anoxic core, compressing their habitat toward the oxic surface. In contrast, late-stage larvae and juveniles may exploit the hypoxic and anoxic core boundaries, and even cross the anoxic core. If deoxygenation results in a vertical expansion of the anoxic core, early larval survival could be compromised, and recruitment of meso-bathypelagic species could decrease. Therefore, it is necessary to understand how fish undergo their larval development in and around hypoxic and anoxic environments.

Studies focusing on fish larvae distributions in OMZs are scarce and mostly restricted to the upper ~ 200 m of the water column. A multiyear time-series in the California Current showed a 63% decrease in abundance of midwater fishes (e.g., *Cyclothone* spp. and *Vinciguerria lucetia*) related to deoxygenation (Koslow et al. 2011). More recent studies have focused on fish larvae distribution and DO gradients in the OMZ off Mexico. Davies et al. (2015) highlighted the high larval abundance of the East Pacific codlet (*Bregmaceros bathymaster*) in upwelled suboxic waters. Sánchez-Velasco et al. (2019, 2022) detected a larval fish species assemblage (e.g., frigate tuna *Auxis* spp.) restricted to oxic waters, and other assemblages (e.g., Diogenes' lanternfish *Diogenichthys laternatus*) with highest abundance in hypoxic to suboxic waters. At the entrance of the Gulf of California, Gutiérrez-Bravo et al. (2022) reported that a strongly stratified water column may favor the northward expansion of the subsurface larval fish assemblage dominated by *D. laternatus*.

Studies with deeper sampling protocols have described the distribution of fish larvae and other zooplankton groups in or below the anoxic core of the ETNP-OMZ. Wishner et al. (2013, 2018) found that in the Costa Rica Thermal Dome (CRTD), where the anoxic core ranged from 300 to 500 m depth, zooplankton below the thermocline accounted for ~ 50% of total biomass. Contrastingly, off central Mexico, where the anoxic core ranged from 150 to 700 m depth, > 75% of the integrated zooplankton biomass was restricted to the thermocline (< 150 m depth). Maas et al. (2014) found that myctophid larvae were constrained to the mixed layer as preflexion larvae, and only later stages (> 22 mm) ventured into the anoxic core during daytime. They also report a diverse adult fish assemblage, dominated by *Cyclothone* spp., below the OMZ lower boundary, at DO > 9 μmol/kg. These reports hint that OMZ-resident species utilize the DO gradients of the core boundaries differently through their development. However, the distribution of life stages is still unclear.

By using horizontal plankton tows to track specific oxypleths across a broad geographical area, this research analyzed the distribution of fish larvae (by species and larval stages) and juveniles in relation to DO concentrations across the ETNP-OMZ. We expected to encounter higher larval abundances in the oxic mixed layer, distinct larval assemblages across the upper and lower OMZ boundaries, and a relatively high abundance of juvenile mesopelagic fish in the lower boundary. Moreover, we expected to observe epipelagic species to be vertically restricted to the oxic surface through their development, and meso-bathypelagic species to present vertical shifts in distribution as they develop into juveniles.

Methods

Satellite images

Daily, L4-processed satellite data were obtained for sea surface temperature (SST, 0.5° resolution), sea level anomaly (SLA, 0.25° resolution), and surface Chlorophyll a (Chl *a*; 4 km resolution) for the duration of the sampling period (December 24, 2021 to January 21, 2022) (Generated using E.U. Copernicus Marine Service Information; SST: https://doi.org/10.48670/moi-00165 SLA: https://doi.org/10.48670/moi-00149 Chlorophyll: https://doi.org/10.48670/moi-00279). The temporal average of the data was calculated and mapped using MATLAB.

On board sampling

An oceanographic survey was performed onboard the RV *Sally Ride* from Puntarenas, Costa Rica to San Diego, USA. Forty-nine CTD-rosette stations and eight nighttime MOCNESS tows (Multiple Opening-Closing Net and Environmental Sensing System; Wiebe et al. 1985) were conducted along the cruise track. Equipment of the CTD-rosette included a *SeaBird SBE9* + CTD and recently calibrated Seapoint-Fluorescence and SBE 43-DO sensors. The MOCNESS was equipped with 10 nets of 1 m^2 mouth opening and 333 μm mesh size, a *SeaBird SBE9* + CTD, a *SeaBird SBE 43* DO sensor, and flow meter and angle sensors.

The MOCNESS tows were performed at locations of particular biological interest (Fig. 1), such as the CRTD (M1), San Jose submarine canyon (M2), the center (M3, M5), and borders (M4, M6) of two anticyclonic eddies (abbreviated ACE-1 and ACE-2), and across the northern portion of the OMZ (M7 and M8).

Using manufacturer software (SBE Data Processing), CTD data were filtered and aligned. CTD-rosette data was binned to 1 m depth and MOCNESS data was binned to 10 s. Conservative Temperature and Absolute Salinity were calculated. CTD-rosette data were used to construct hydrographic sections, while MOCNESS sensor data were used to describe the environmental conditions of zooplankton samples.

The MOCNESS tows were performed at 1.5–2 knots net speed and at 40°–50° net angle. A horizontal net tow strategy was followed to sample selected DO concentrations (oxypleths) in five sampling levels: (1) the oxic level (~ 200 μmol/kg, near surface), (2) the hypoxic (~ 100 μmol/kg), and (3) suboxic (~ 10 μmol/kg) levels in the upper core boundary, (4) the anoxic core level (< 1 μmol/kg, at the center of the anoxic core), and (5) the deep level (~ 10 μmol/kg in the lower boundary below the anoxic core). The remaining five MONCESS nets were opened during transitions between target depths and were not used for this study. This horizontal sampling protocol allows for discrete, punctual sampling events, but cannot provide continuous, vertically integrated abundances as oblique tows would (Wiebe et al. 2015). An example of the configuration of horizontal sampling levels along the water column is shown in Fig. 2.

The oxic, hypoxic, and suboxic levels were sampled for ~ 10 min (~ 500 m^3 filtered volume). The deep and anoxic levels were sampled for ~ 20 min (~ 1000 m^3 filtered volume) to obtain sufficient sample material. Due to time constraints and to eliminate any differences between stations caused by the phase of diel vertical migration, all the net deployments were performed during nighttime. Hence, the sampling results reflect nighttime distributions only.

Sample handling

Gelatinous organisms, nonplanktonic groups and excess water were removed from the samples after they were retrieved from the cod ends. The samples were preserved with Ethanol 96%. At least two ethanol changes were performed during the cruise and a third was performed on land.

Zooplankton biovolume was measured by the displacement method (Steedman 1976) and standardized to mL/1000 m^3 by dividing the zooplankton displacement volume (mL) by the volume of water filtered by the net (m^3).

Fish larvae and juveniles were separated and counted under a stereoscope. Fish larvae were identified to the most specific taxonomic level possible, using specialized bibliography (Evseenko 1990; Moser 1996; Aceves-Medina et al. 1999, 2003; Evseenko and Shtaut 2000; Richards 2005; Jiménez-Rosenberg et al. 2006; González-Navarro et al. 2013; Silva-Segundo et al. 2021). The larval stages (preflexion, flexion, postflexion, and transformation) were defined according to Moser (1996). Preflexion and flexion larvae were considered "early larval stages" as they both lack fully developed fins. Larval abundances were standardized to larvae/1000 m^3 and were considered absolute abundances.

Juveniles and adults were separated, counted, and identified to family level, except for the Gonostomatidae, that were represented entirely by the genus *Cyclothone*. Adult abundances were standardized to fish/1000 m^3. Because the increased swimming ability of adult fish could affect fishing efficiency, abundances were considered relative, and should not be compared with the absolute abundances of fish larvae.

The hydrographic and biological data will be uploaded to the BCO-DMO repository under the project "Collaborative

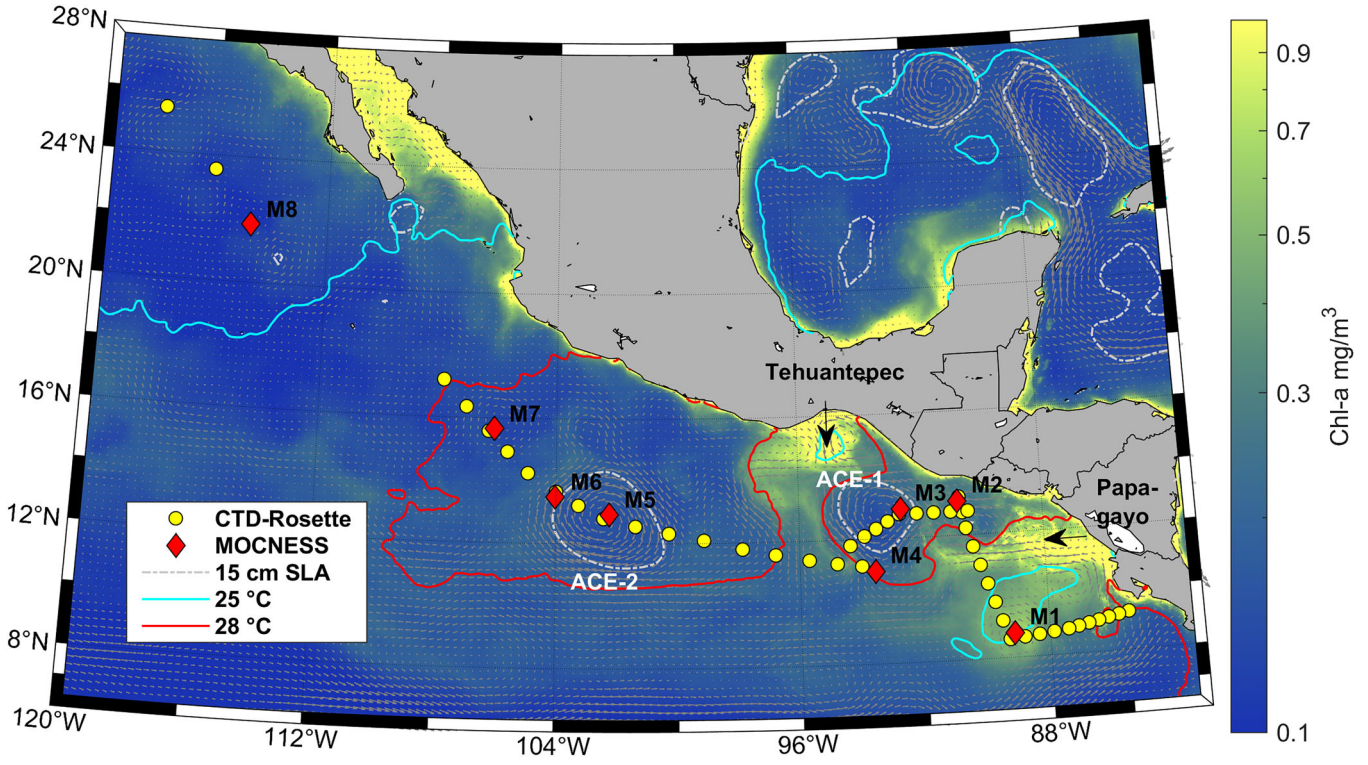

Fig. 1. Study area. Colored background indicates surface Chl *a* (mg/m^3) averaged for the duration of the cruise. Red diamonds indicate MOCNESS Sta. (M1–M8). Yellow Circles indicate CTD stations. Light gray contours encircle a 15 cm positive SLA, indicative of anticyclonic eddies (ACE). The 25°C and 28°C isotherms are highlighted as blue and red contours, respectively.

research: Multiyear autonomous measurement of N-loss in the ETNP ODZ", and are also available by email request.

Statistical analysis

The DO range sampled by each net was calculated. Nets that sampled at less than half or more than double the desired DO value were excluded from the analyses that compared sampling levels.

The mean and standard deviation of zooplankton biomass and larval abundance were calculated for each sampling level. A battery of non-parametric Kruskal-Wallis and Mann–Whitney tests (Campbell et al. 1970) were performed to assess the significance of differences in biovolume and larval abundance among levels. Olmstead Tukey tests were used to classify species as dominant, constant, occasional, and rare according to their larval abundance and frequency of occurrence (Sokal and Rohlf 1995) in each sampling level. The adult habitats of the most abundant species were consulted in FishBase (Froese and Pauly 2010). A Chi-squared test (Villarroel del Pino 2018) was conducted to determine if the distribution of larval development stages was independent of the sampling level. Two canonical correspondence analyses (CCA, Ter Braak 1986; Dixon 2003) were conducted to better understand the variations of species and larval development stages in relation to environmental variables (DO, Conservative Temperature, Absolute Salinity, Biovolume).

Results

Satellite images

A synoptic view of the satellite data is shown on Fig. 1. Chlorophyll *a* data shows eutrophic (> 0.5 mg/m^3) surface waters in coastal waters, along the wind jets of Tehuantepec and Papagayo, and in the CRTD. Oligotrophic conditions (~ 0.1 mg/m^3) are seen in oceanic waters, particularly in ACE-1 and ACE-2. The warmest (> 28°C) waters were observed along the Central American and Mexican coasts, and in ACE-1 and ACE-2. The coldest (< 25°C) waters were present north of ~ 20° latitude, and in localized pockets at the CRTD and the Tehuantepec wind jet. Strong currents were observed seaward of the wind jets and around ACE-1 and ACE-2.

Hydrography

The mixed layer depth varied along the cruise track, as seen by conservative temperature and the 24 kg/m^3 isopycnal (Fig. 3a). Near Costa Rica (hydrographic stations before M1), the mixed layer was ~ 35 m depth. At the CRTD (Sta. M1), the mixed layer was < 10 m depth. Near Guatemala (Sta. M2–M4), the mixed layer sunk to > 40 m depth, reaching 75 m within the ACE-1 around Sta. M3. The mixed layer shoaled to ~ 25 m

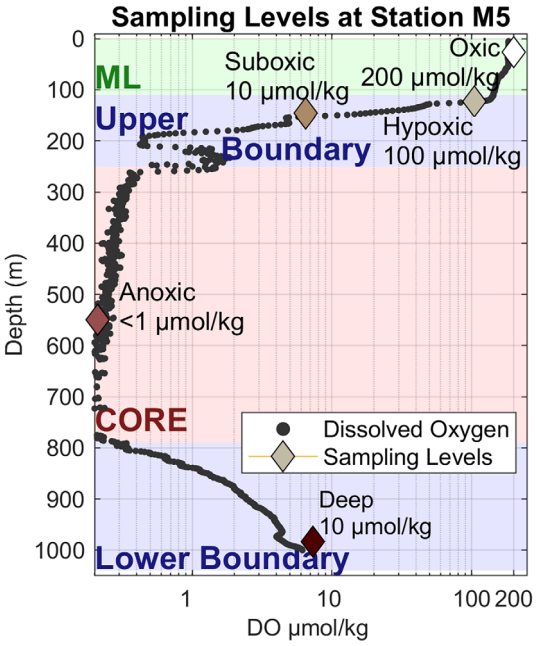

Fig. 2. Vertical configuration of the five sampling levels. Sta. M5 is used as an example. The vertical profile of DO (μmol/kg) is shown by gray circles. The depth and DO of each sampling level (oxic, hypoxic, suboxic, anoxic, and deep) is indicated by color-coded diamonds. The distinct vertical sections in the profile are color-shaded (mixed layer as green, upper-lower core boundaries as blue, and anoxic core as red).

in the Tehuantepec wind jet. Off central Mexico, the mixed layer expanded to ~ 60 m depth, with a maximum depth of ~ 130 m inside the ACE-2. In the northern Sta. M7 and M8, the mixed layer depth remained ~ 60 m.

The vertical extent of the oxic layer (between the surface and the 100 μmol/kg oxypleth) roughly followed the 24 kg/m^3 isopycnal (Fig. 3b). Off Central America, the oxic layer expanded to ~ 75 m depth around the ACE-1, and contracted to 10 and 20 m depth in the CRTD and the Tehuantepec wind jet, respectively. Off central Mexico, the oxic layer was thicker (~ 120 m). North of Sta. M7, the oxic layer expanded deeper than the 24 kg/m^3 isopycnal and reached DO values > 200 μmol/kg.

The hypoxic (100–10 μmol/kg) and suboxic (10–1 μmol/kg) layers in the upper core boundary were not associated to isopycnal surfaces. The hypoxic layer reached its greatest vertical extent (250 m) around the CRTD. Then, it gradually shoaled to ~ 50 m depth in the Tehuantepec wind jet, where its extent decreased to ~ 30 m. The hypoxic layer remained ~ 30 m thick in the stations off central Mexico, but gradually expanded again in the northern section of the study area, reaching > 300 m depth north of Sta. M8. The vertical extent of the suboxic layer was also greater in the CRTD and south of Tehuantepec (~ 100 m) than off central Mexico (~ 30 m). Broad (100–200 vertical m) suboxic intrusions were observed in the peripheries of ACE-1 and ACE-2.

Anoxic waters gradually shoaled from 350 to 200 m depth between Sta. M1 and M4, and reached their shallowest extent (100 m depth) off central Mexico. The deepest extent of anoxic waters also increased from Sta. M1 (550 m) to Sta. M4–M7 (~ 850 m), resulting in anoxic waters extending vertically for 750 m off central Mexico. However, at Sta. M8, the anoxic core had contracted to 250–600 m depth and was discontinuous, with a suboxic intrusion between 340 and 470 m. Anoxic waters disappeared at the last hydrographic station (25°N).

In the lower core boundary, a deep suboxic layer (1–10 μmol/kg) of ~ 200 m thickness was observed. DO concentrations > 10 μmol/kg below the anoxic core were seen at the southern and northern sections of the cruise track.

MOCNESS sampling strategy

The five sampling levels generally followed the desired oxypleths and the desired horizontal sampling strategy (Table 1). Abrupt vertical oxygen gradients and the lagged depth control of the MOCNESS tow caused DO values to be less than half or more than double the desired values in 7 out of 40 nets (M1-Oxic, M1-Hypoxic, M6-Hypoxic, M3-Suboxic, M6-Suboxic, M7-Suboxic, and M8-Anoxic). DO also varied within each individual net tow (Supporting Information Data S1).

Zooplankton biovolume and larval abundance

In general, zooplankton biovolume decreased gradually from the oxic to the anoxic level, and increased again at the deep level (Fig. 3a, Supporting Information Data S2). Notably, the zooplankton biovolume of the suboxic level was greater than that of the deep level, although both levels sampled at 10 μmol/kg oxypleth.

A total of 3732 fish larvae were counted. Larval abundance is shown in Fig. 3b and Supporting Information Data S2. There were significant differences in larval abundance between oxygen sampling levels (Kruskal-Wallis test, $P < 0.001$). High larval abundances (> 200 larvae/1000 m^3) were observed in the oxic and hypoxic levels. Moderate larval abundances were observed in the deep and suboxic levels (17 and 7 larvae/1000 m^3, respectively). The lowest larval abundances were observed in the anoxic level (< 1 larvae/1000 m^3).

Zooplankton biovolume and larval abundance also varied between stations (Fig. 3). Sta. M2 (San Jose canyon), M4 and M6 (edges of ACE-1 and ACE-2) had the highest zooplankton biovolumes and larval abundances, while M3 and M5 (centers of ACE-1 and ACE-2) had lower zooplankton biovolume and larval abundances. Sta. M2–M4, near the Central American coasts, generally had higher zooplankton biovolume and larval abundances than Sta. M5–M7 off the coast of central Mexico.

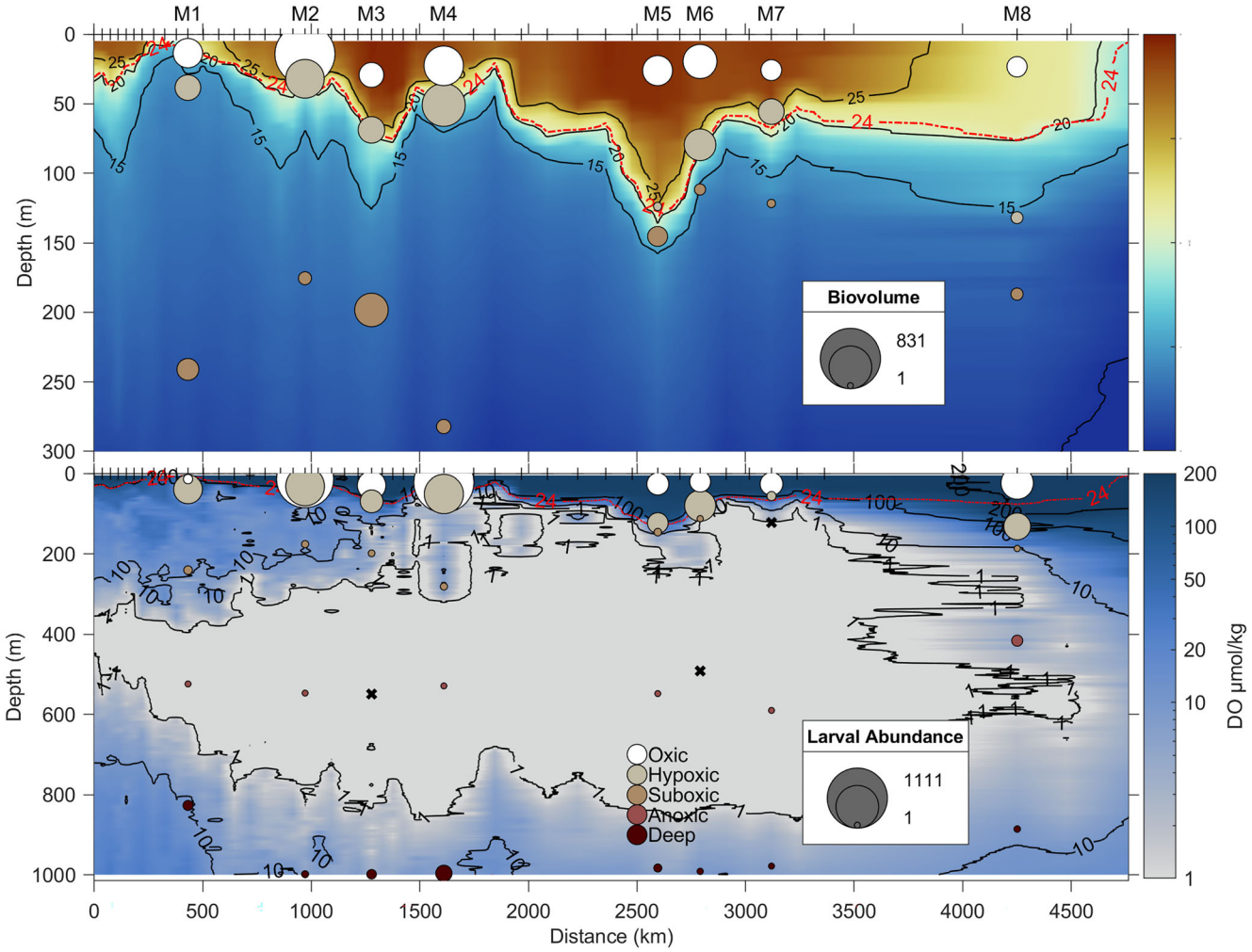

Fig. 3. Hydrographic sections of Conservative Temperature (**a**, 0–300 m depth) and DO (**b**, 0–1000 m depth) along the cruise track. The x axis indicates traveled distance. The y axis indicates depth. The dashed red lines indicate the 24 kg/m^3 isopycnal. Zooplankton biovolume (mL/1000 m^3, panel a) and larval abundance (larvae/1000 m^3, panel b) are indicated by bubble size, and sampling level is indicated by bubble color. *X* symbols indicate zero abundance. DO is shown on logarithmic color scale (a non-log view is shown on Supporting Information Data S6).

Fish larvae community structure

The total fish larvae taxonomic richness was 92 taxa. The sampling levels with highest species richness were the oxic (64 taxa) and hypoxic (49 taxa) levels. The 11 most abundant taxa (presented on Table 2) accounted for 89.5% of the total larval abundance. The adult habitats of the 11 taxa in Table 2 were mesopelagic (5 taxa), demersal (3 taxa), epipelagic (2 taxa), and bathypelagic (1 taxon).

The three most abundant species *D. laternatus* (Myctophidae), *Benthosema panamense* (Myctophidae) and *V. lucetia* (Phosichthyidae) were of mesopelagic adult habitat.

The Olmstead-Tukey analyses performed on each sampling level highlighted patterns in taxon distribution (Table 2). *Opisthonema* spp. (Clupeidae), *Dormitator latifrons* (Eleotridae), *Diaphus pacificus* (Myctophidae), and *Auxis* spp. (Scombridae), were dominant only in the oxic level. *Ophidion* spp. (Ophidiidae) and *B. bathymaster* (Bregmacerotidae) were dominant only in the hypoxic level. *Benthosema panamense* and *V. lucetia* were dominant in the oxic and hypoxic levels. *Diogenichthys laternatus* was dominant in the hypoxic and deep levels. No species were dominant in the suboxic and anoxic levels, but *D. laternatus* and *V. lucetia* were constant in both, and *Cyclothone* spp. was constant in the anoxic and deep levels.

The distribution of the two most frequently occurring species, *D. laternatus* and *V. lucetia*, is shown in Fig. 4. The distribution of all other dominant species is presented as Supporting Information Data S3, S4, and S5. *D. laternatus*, the most abundant species overall, was distributed across all five sampling strata (ranging from 15 to 1027 m depth) and showed a preferential habitat for hypoxic waters. *V. lucetia* also showed a wide depth range (15–999 m) but was more abundant in the upper oxic and hypoxic levels, with very low abundances (< 1 larvae/1000 m^3) in the remaining deeper levels and a preferential habitat for oxic waters.

Table 1. Depth (m) and DO (μmol/kg) of individual net tows and sampling levels. Bold values indicate nets with major discrepancies (less than half or more than double the desired DO values) that are excluded from the mean and standard deviation (SD).

			Upper boundary		Lower B
M #	Oxic	Hypoxic	Suboxic	Anoxic	Deep
	Avg. (range)	Avg. (range)	Avg. (range)	Avg. (range)	Avg. (range)
Depth					
M1	**14 (16–0)**	**38 (40–38)**	241 (248–237)	525 (527–521)	827 (834–820)
M2	14 (15–0)	32 (33–31)	175 (176–175)	547 (549–546)	1004 (1008–998)
M3	29 (46–0)	69 (70–68)	**198 (199–198)**	550 (553–547)	1033 (1037–1026)
M4	23 (25–0)	51 (55–49)	282 (285–279)	529 (532–528)	996 (999–991)
M5	26 (30–0)	124 (125–122)	145 (146–145)	549 (550–547)	983 (990–975)
M6	20 (31–0)	**80 (92–70)**	**112 (112–111)**	492 (497–486)	992 (998–985)
M7	26 (32–0)	56 (57–54)	**122 (125–120)**	590 (597–587)	978 (981–974)
M8	23 (34–0)	132 (133–131)	187 (188–185)	**416 (425–409)**	886 (897–879)
Mean	23	77	206	540	962
SD	4.6	37	49	28	65
DO					
M1	**104 (92–156)**	**29 (22–49)**	8 (6–12)	0.2 (0–0.5)	11 (10–13)
M2	217 (213–225)	77 (69–83)	8 (8–10)	0.3 (0–1.1)	8 (7–9)
M3	204 (197–212)	65 (61–75)	**22 (21–24)**	0.2 (0–0.7)	8 (7–9)
M4	201 (194–212)	92 (76–99)	9 (8–10)	0.2 (0.1–0.3)	7 (6–7)
M5	201 (200–203)	105 (80–123)	7 (6–7)	0.2 (0–0.4)	7 (6–8)
M6	204 (201–206)	**86 (34–136)**	**0.3 (0.2–0.4)**	0.3 (0–0.8)	9 (8–9)
M7	202 (195–204)	125 (116–133)	**0.2 (0–0.4)**	0.3 (0–1.2)	8 (6–11)
M8	224 (222–227)	82 (70–92)	10 (6–15)	**1.5 (0–5.2)**	9 (8–10)
Mean	207	91	8.4	0.2	8.3
SD	8.7	20	1.2	0.1	1.1

Table 2. Characterization of dominant species: Adult habitats (E: epipelagic, M: mesopelagic, B: bathypelagic, D: demersal), average larval abundance (Avg. Ab.), Frequency of Occurrence (F.O., %), weighted mean and range of DO (μmol/kg) and depth (meters) and Olmstead-Tukey hierarchies (D: dominant, C: constant, O: occasional, R: rare, X: zero abundance).

						Olmstead-Tukey hierarchies			
Species	Hab	Avg. ab.	F.O. %	DO (range)	Depth (range)	Oxic	Hypoxic	Suboxic	Anoxic	Deep
D. Laternatus	M	856	65	73 (0.2–224)	134 (15–1027)	C	D	C	C	D
B. Panamense	M	221	17.5	194 (8.2–217)	24 (15–999)	D	D	R	X	R
V. Lucetia	M	422	52.5	186 (0.2–224)	47 (15–999)	D	D	C	C	R
Opisthonema spp.	E	78	17.5	216 (201–217)	15 (15–29)	D	X	X	X	X
D. Pacificus	M	77	25	165 (0.3–224)	48 (25–588)	D	C	R	R	X
D. Latifrons	D	58	27.5	194 (9–224)	27 (15–279)	D	C	R	X	X
Auxis spp.	E	20	15	208 (201–217)	24 (15–30)	D	X	X	X	X
Ophidion spp.	D	7	7.5	79 (65–217)	34 (15–69)	R	D	X	X	X
Cyclothone spp.	B	9	17.5	4 (1.5–9)	648 (145–1027)	X	X	R	O	C
Syacium spp.	D	3	7.5	211 (201–217)	18 (15–28)	C	X	X	X	X
B. Bathymaster	M	5	12.5	76 (8.2–204)	69 (28–175)	R	D	R	X	X

Cyclothone spp. showed a strong preference for deep, cold, suboxic waters. With a mean DO concentration of 4 (1.5–9) μmol/kg, the lowest for all the species by more than an order of magnitude, this species was observed below the OMZ anoxic core at all stations.

Some trends in species distribution were observed along the study area, particularly in the oxic and hypoxic levels. In general, Sta. M2–M4 (Central America) had higher larval abundances and taxonomic richness than Sta. M5–M7 (Mexico), further off the coast. Taxonomic richness at Sta. M2–M4 was

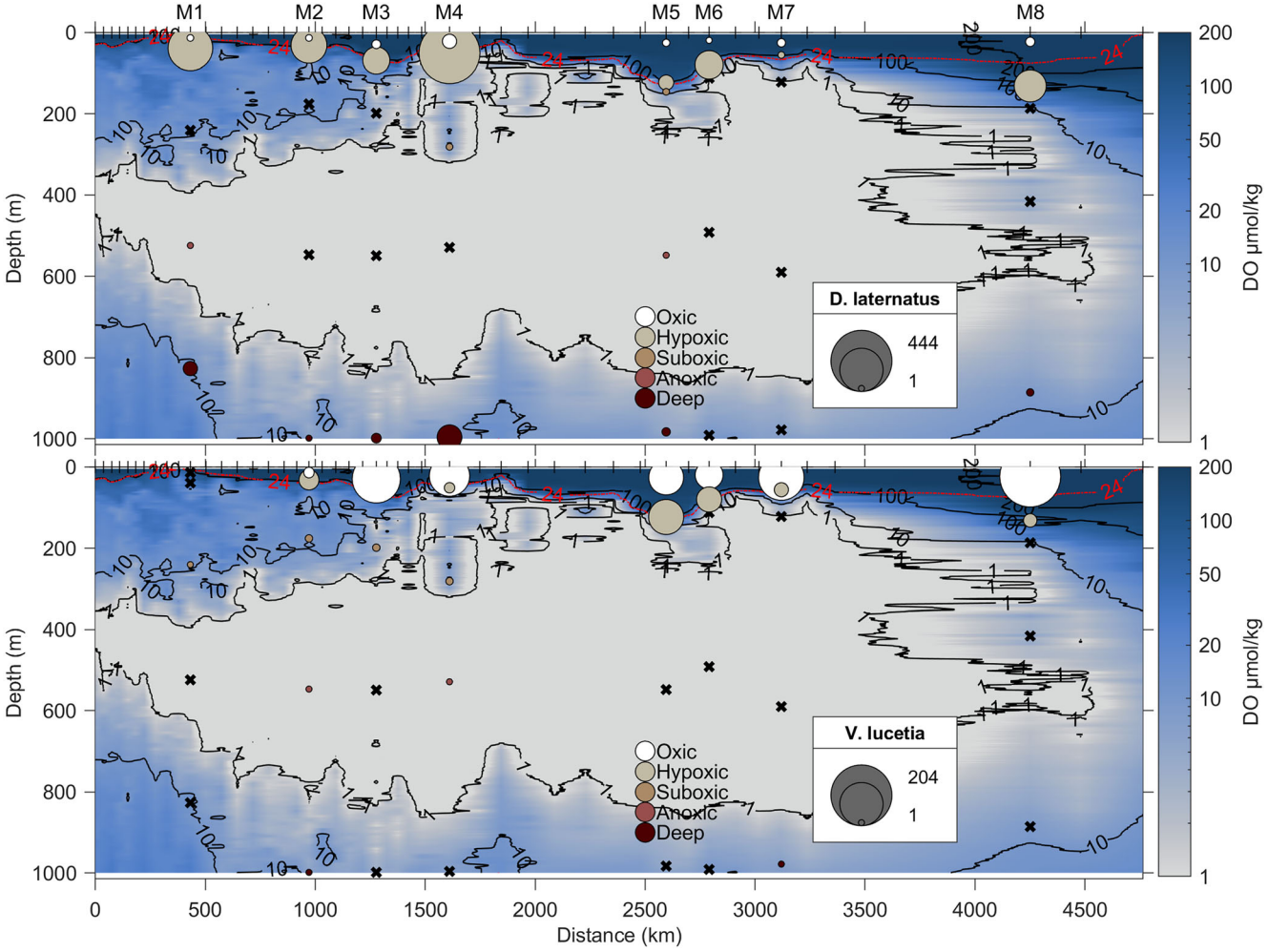

Fig. 4. Distribution of the most frequently occurring fish larvae, *D. laternatus* (top) and *V. lucetia* (bottom). The x axis indicates distance traveled. The y axis indicates depth. DO is shown on logarithmic color scale. The red dashed line indicates the 24 kg/m^3 isopycnal. Larval abundance (larvae/1000 m^3) is indicated by bubble sizes, while sampling level is indicated by bubble color. *X* symbols indicate zero abundance.

49 taxa in the oxic level and 33 taxa in the hypoxic level, while at Sta. M5–M7 taxonomic richness decreased to 29 taxa in the oxic level and 20 taxa in the hypoxic level. Dominant species *B. panamense* and *Ophidion* spp. were present only at Sta. M2–M4, while other dominant taxa were present throughout the sampling area.

Distribution of developmental stages

Early (preflexion plus flexion) and postflexion stages were the most abundant developmental stage, accounting for 34% and 51% of the total standardized larval abundance, respectively. The transformation stage accounted for 15% of the larval abundance.

The chi-squared test results ($X^2_{8,702} = 141.06$, $p < 0.001$) indicated that the distribution of larval stages was dependent on oxygen sampling level. Over 85% of the standardized abundance of early stages was in the oxic level, and early stages were almost absent from the suboxic, anoxic, and deep levels. Postflexion and transformation stages were also most abundant in the oxic and hypoxic levels, but were also present in the suboxic, anoxic, and deep levels, although at lower abundances (Fig. 5).

The distribution of larval development stages varied with the adult habitat of each species (Fig. 6). All the larval development stages of epipelagic species (*Auxis* spp. and *Opisthonema* spp.) were restricted to the oxic level. Early and postflexion stages of demersal species (*D. latifrons*, *Syacium* spp.) were distributed in the oxic and hypoxic levels. Early stages of mesopelagic species (*D. laternatus*, *B. panamense*, *V. lucetia*, *D. pacificus*, and *B. bathymaster*) were most abundant in the oxic level, while postflexion stages were most abundant in the hypoxic level, with a modest mean abundance (14 larvae/1000 m^3) in the deep level. The sole bathypelagic taxon *Cyclothone* spp. was only present as transformation larvae,

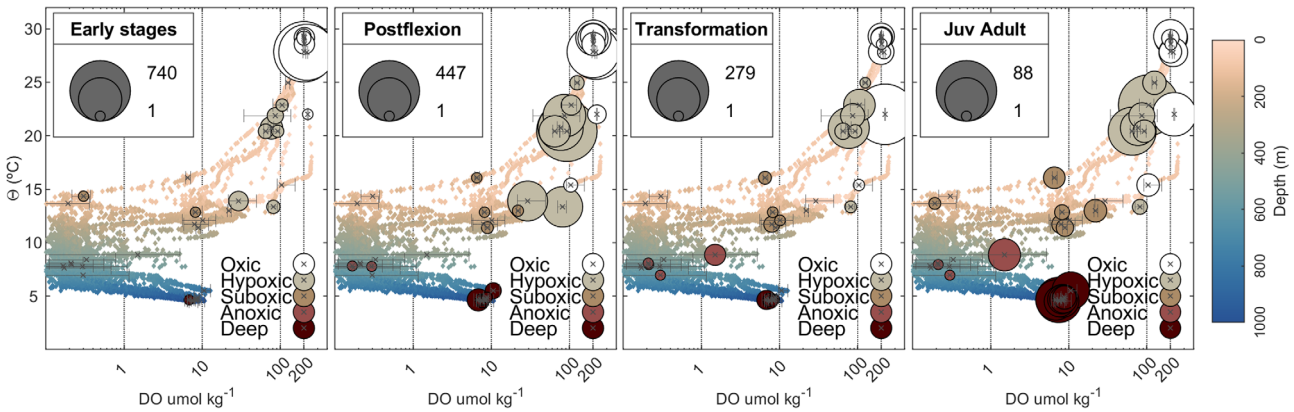

Fig. 5. Distribution of development stages in conservative temperature-log DO space. The diagrams show MOCNESS DO profiles (scatter plot) superimposed by abundances (bubble plot) of the dominant species' four development stages (from left to right: early stages [preflexion and flexion], postflexion, transformation, and juvenile/adult). The size of the bubbles indicates larval abundance, and the color indicates sampling level. *X* symbols indicate average DO concentration, and horizontal lines indicate DO range within each sample.

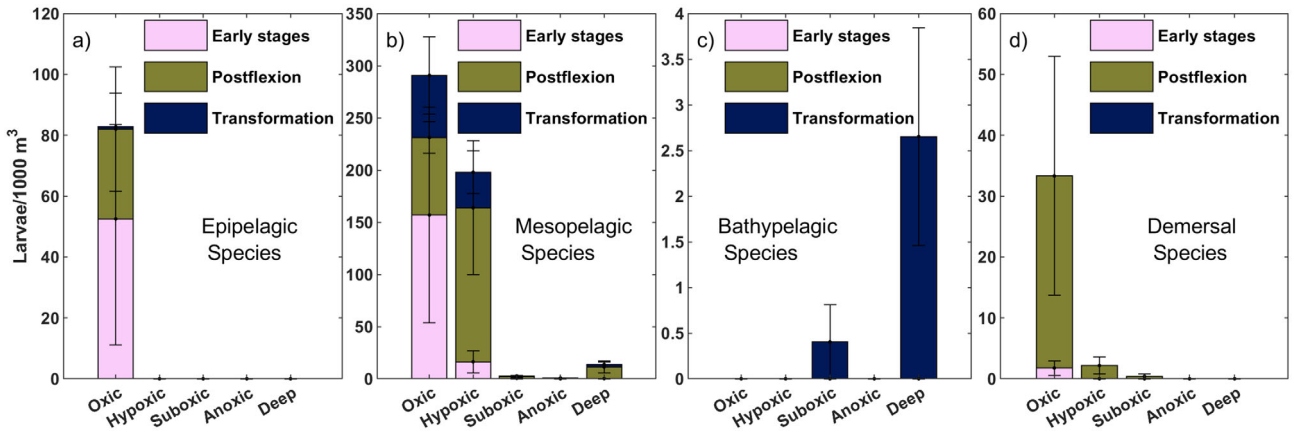

Fig. 6. Mean larval abundance of developmental stages across the five sampling levels. Error bars indicate standard error.

with highest abundances in the deep level and in M8-Anoxic, where DO = 1.5 (0–5.2) μmol/kg.

Distribution of juveniles and adults

A total of 515 fish juveniles and adults were caught. The highest relative abundances (mean ± standard error) were observed in the hypoxic (35.6 ± 14.6 fish/1000 m^3), deep (26.7 ± 4.3 fish/1000 m^3), and oxic (17.2 ± 5.2 fish/1000 m^3) levels, while the suboxic and anoxic levels had a mean abundance of < 1 fish/1000 m^3. The distribution of the most abundant fish families, Gonostomatidae (*Cyclothone* spp.), Myctophidae, and Phosichthyidae are shown in Fig. 7. Gonostomatidae were most abundant in the deep level (24.6 ± 4.6 fish/1000 m^3). Myctophidae were more abundant in the hypoxic level (14.3 ± 6.4 fish/1000 m^3), but were also present in the oxic and deep levels. Phosichthyidae were most abundant in the hypoxic (5.2 ± 3.4 fish/1000 m^3) and oxic (5.2 ± 3.4 fish/1000 m^3) levels, and were absent from the anoxic and deep levels.

Fish larvae ecological relations

The CCA explained 55.9% of the variance in development stages' distribution, and 37.9% of the variance in dominant species. The most explanatory variable in both CCAs was DO.

The CCA results on larval development stages (Fig. 8a) show a transition from a positive correlation with DO, conservative temperature, and biovolume in early stages to a negative correlation in the postflexion and transformation stages.

The CCA results on dominant species (Fig. 8b) showed that *Cyclothone* spp., *D. laternatus*, *B. bathymaster*, and *Ophidion* spp. were negatively correlated with DO and temperature, but positively correlated with Absolute Salinity. In contrast, *Auxis* spp., *D. latifrons*, *B. panamense*, *Syacium* spp., and *Opisthonema* spp. were positively correlated with DO, Conservative

Temperature, and zooplankton biovolume. *D. pacificus* and *V. lucetia* were negatively correlated with biovolume.

Discussion

Our results revealed important aspects of the three-dimensional distribution of fish larvae and juveniles in relation to DO gradients across the ETNP-OMZ, from 0 to 1000 m depth and from the CRTD to the Southern California Current, during hours of darkness. The oceanographic characteristics of this extensive region were variable, but the presence of a wide anoxic core in the intermediate water triggered characteristic ecological responses in the larval fish community. Although this study was based on only nocturnal samples, the findings indicated that vertical DO structure is a determinant factor in the distribution and survival of fish larvae.

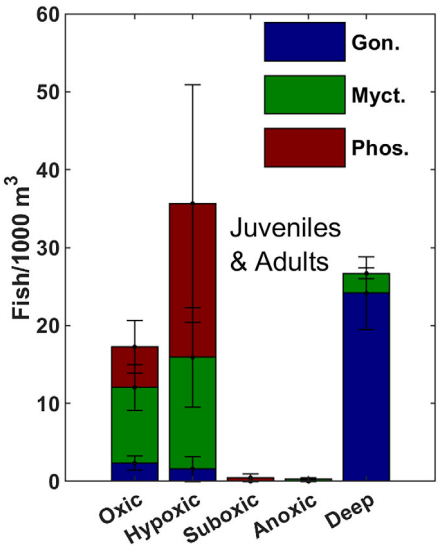

Fig. 7. Mean abundance of juvenile and adult fish of the most abundant families (Gonostomatidae, Myctophidae, and Phosichthyidae) across the five sampling levels. Error bars indicate standard error.

Oxygen variability in the ETNP-OMZ

Despite the great distance that existed in sampling stations, the oxygen variability along the cruise track describes the anatomy of the OMZ anoxic core from the south (Costa Rica Dome) to the north (Southern California Current). Our results highlighted the high hydrographic variability, possibly due to mesoscale processes, between the CRTD and the Gulf of Tehuantepec, and indicated that the understudied Central American coasts were more oxygen-depleted than what is reported in climatologies (Garcia et al. 2019) and recent interpolations based on climatological means (Kwiecinski and Babbin 2021). The World Ocean Atlas Garcia et al. (2019) presents minimum values of $\sim 3\ \mu$mol/kg and waters $< 10\ \mu$mol/kg only below 400 m depth. We observed an anoxic core ($< 1\ \mu$mol/kg) from 200 to 800 m depth across the warm waters southeast of the Tehuantepec wind jet. This discrepancy highlights the need for more direct measurements in this understudied region.

The shallow (~ 100 m) anoxic core observed off central Mexico (between 16°N and 20°N) and its subsequent vertical contraction between 20°N and 23°N display how intrusions from the California Current in this northern boundary of the OMZ increase subsurface oxygen content (Cepeda-Morales et al. 2013). The suboxic intrusion observed at 340–470 m depth around Sta. M8 is an example of the deep intrusions that are statistically described by Kwiecinski and Babbin (2021), and corroborated here.

Horizontal distribution of fish larvae

Considering that all biological samples were collected at night, the community of fish larvae is comparable between stations. The high larval fish abundances at Sta. M2 (e.g., 999 larvae/1000 m^3 at the oxic level), dominated by the neritic

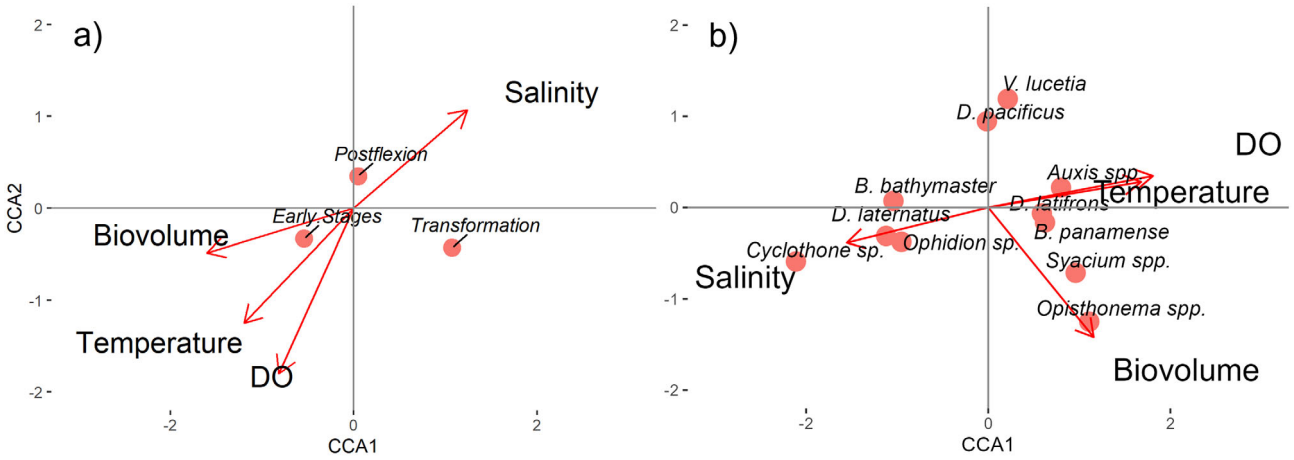

Fig. 8. CCA results for larval development stages (**a**) and dominant species (**b**).

Opisthonema spp. and the mesopelagic *B. panamense*, was consistent with the location proximal to shore and in San Jose submarine canyon, a geological feature of high biological activity (Quintana-Rizzo et al. 2021).

The high larval abundance of Sta. M4 (1111 larvae/1000 m^3 at the oxic level), comprised mostly of *B. panamense*, a species of eutrophic-water affinity (Davies et al. 2015; Gutiérrez-Bravo et al. 2022) is consistent with its location in the high-chlorophyll frontal current on the edge of ACE-1. The biological variability between Sta. M2 and M4 is in line with the habitat diversity due to high mesoscale activity between the CRTD and Tehuantepec during winter (Fiedler and Lavín 2017).

The most abundant species in Sta. M5 (center of ACE-2) was *V. lucetia*, comprising 47% of the total larval abundance in the station. This agrees with reports of the species being dominant in thick oligotrophic mixed layers (Davies et al. 2015; Gutiérrez-Bravo et al. 2022). Contrastingly, the most abundant species in the shallow hypoxic conditions of Sta. M6 (edge of ACE-2) were the myctophids *D. laternatus* (34%) and *D. pacificus*, comprising 34% and 15% of the total larval abundance in the station (15%).

The northern Sta. M7 and M8 had relatively low zooplankton biovolume (< 150 mL/1000 m^3), high larval abundances (> 100 larvae/1000 m^3) of *V. lucetia* in the oxic level and *D. laternatus* in the hypoxic level, and absence of tropical species observed in southern stations. These characteristics are similar to the previously described "Transitional-California Current" larval fish habitat (Leon-Chávez et al. 2015), in agreement with the subtropical nature of the northern limit of the ETNP-OMZ.

Vertical distribution of dominant species

The nighttime larval distribution of the dominant species in this study may have described a shallower distribution range, depending on the species' vertical migration patterns. However, our sampling strategy compared nocturnal abundances exclusively for the first time, unlike most previous studies of fish larvae at the entrance of the Gulf of California (e.g., Davies et al., 2015; Sánchez-Velasco et al., 2019; Gutiérrez-Bravo et al., 2022) where diurnal and nocturnal abundances are compared indiscriminately.

From these previous studies, it was known that epipelagic species, namely *Auxis* spp., were restricted to the warm oxic layer (Sánchez-Velasco et al. 2019). This study showed that epipelagic species undergo their whole larval development in this layer.

Bregmaceros bathymaster was abundant in coastal hypoxic waters, consistent with previous reports (Davies et al. 2015). On the other hand, *D. laternatus* observed a wide vertical distribution across the sampling area, corroborating its use as bioindicator of anoxic subsurface environments in the ETNP-OMZ (Sutton et al. 2017; Reygondeau et al. 2018). Though both *B. bathymaster* and *D. laternatus* thrive in low-oxygen environments, they display distinct ecological adaptations: *B. bathymaster* is abundant in shallow hypoxic conditions related to coastal upwelling, while *D. laternatus* is abundant in subsurface suboxic to anoxic conditions related to strong stratification.

The distribution of demersal species *Ophidion* spp. and *D. latifrons* in hypoxic waters was unexpected and in contrast with the hypoxia-restricted demersal flatfish *Syacium* spp. *Ophidion* spp. and *D. latifrons* are coastal species that inhabit soft-bottom habitats, sometimes in brackish water (Robertson and Allen 2008), where hypoxic conditions are common (Breitburg et al. 2018). Our results indicated that, while some demersal species inhabit solely in the oxic mixed layer, other hypoxia-tolerant species can inhabit deeper layers during their larval phases.

Finally, the high abundances of transformation larvae and adults of *Cyclothone* spp. in the lower core boundary agree with previous reports (Wishner et al. 2013; Maas et al. 2014) of a resident zooplankton community with the highest biomass observed at DO ~ 2 μmol/kg below the anoxic core, comprised of *Cyclothone* spp. and *Gennadas* spp. shrimp. In this biomass peak, Maas et al. (2014) report *Cyclothone* spp. (> 22 mm) abundances of 1700 ind./1000 m^3, while we observed abundances of ~ 24 adults/1000 m^3. It appears that the abundance of this bathypelagic taxon varies sharply along the lower core boundary, and high-abundance layers are present at specific oxypleths. Further sampling effort, with a fine vertical resolution, is required to resolve the distribution patterns of this lower core boundary community.

Trends in larval fish development

There is a generalized trend of hypoxia avoidance during the first preflexion and flexion larval stages, followed by greater hypoxia tolerance during later larval stages. This pattern can be attributed to the superior capacity of larger organisms to withstand an anaerobic metabolism for extended periods of time (Nilsson and Östlund-Nilsson 2008). However, the sharp decrease in larval fish abundance observed in the suboxic and anoxic levels indicates that most fish larvae, even in advanced larval stages, do not live at DO levels < 10 μmol/kg, with some exceptions like *Cyclothone* spp. and *D. laternatus*.

This increased hypoxia tolerance of late larval stages can serve species differently: for mesopelagic species, like *B. panamense*, *V. lucetia*, and *Diaphus pacificus*, the enhanced hypoxia tolerance may allow diel vertical migrations into aphotic depths safe from visual predation during daytime. For species that appear to cross the anoxic core, like *D. laternatus* or *Cyclothone* spp., the increased hypoxia tolerance may also allow them to prey on the bathypelagic zooplankton of the lower core boundary. Comparing daytime and nighttime distributions of larval stages would differentiate between these vertical movements of larvae across the anoxic core and its boundaries.

Ecological and management implications

Despite the small number of biological sampling stations and CTD casts in a wide region of the Pacific, our results suggest a greater oxygen depletion than what is reported in previous studies (Fiedler and Talley 2006; Garcia et al. 2019; Kwiecinski and Babbin 2021). As larval fish abundances decreased sharply in the suboxic (< 10 larvae/1000 m^3) and anoxic (< 1 larvae/1000 m^3) levels, a detrimental effect on fish abundance is expected if deoxygenation trends continue.

The vertical distribution of fish larvae responded to the DO gradients, and varied by development stage and by the species' adult habitat. Therefore, a vertical expansion of anoxic and suboxic waters could disrupt the current vertical zonation of species and development stages. Epipelagic species of commercial importance (i.e., *Auxis* spp., *Opisthonema* spp.) would be vertically restricted to a shoaling oxic layer throughout their development (e.g., Sánchez-Velasco et al., 2019). Mesopelagic species would also be displaced to shallower depths, increasing habitat overlap with epipelagic taxa and implying a restructuring of the larval fish community. Contrarily, bathypelagic species would be displaced to greater depths, hampering their vertical movements and the carbon-exporting linkage between the epipelagic and bathypelagic ecosystems (Archibald et al. 2019). This evidence illustrates a critical panorama for the pelagic fish of the ETNP-OMZ and the associated ecosystem functions and fisheries productivity.

Conclusion

This study was supported by few sampling stations in a wide geographic region, with sample collection occurring only during nighttime. However, we consider our findings highly relevant.

The OMZ anoxic core was almost devoid of fish larvae, with abundances of < 1 larvae/1000 m^3. This feature constrained the habitat of all stages of epipelagic larvae (*Auxis* spp.), and early stages of mesopelagic larvae (*B. panamense*). It appears that only late larval stages and juveniles of mesopelagic (*D. laternatus*) and bathypelagic (*Cyclothone* spp.) species can cross the anoxic core. Although some species (e.g., *Ophidion* spp., *B. bathymaster*) were abundant in the hypoxic environment of the upper core boundary, fish larvae appear to be less tolerant to suboxic (< 10 μmol/kg) conditions than invertebrate zooplankton groups. With the observed trends of deoxygenation, our results indicate that a vertical expansion of anoxic waters would detrimentally affect the development and community structure of fish in the ETNP, with unpredictable effects on fisheries and ecosystem function.

Data availability statement

The hydrographic and biological data will be uploaded to the BCO-DMO repository under the project "Collaborative research: Multiyear autonomous measurement of N-loss in the ETNP ODZ" upon project completion.

References

Abdel-Tawwab, M., M. N. Monier, S. H. Hoseinifar, and C. Faggio. 2019. Fish response to hypoxia stress: Growth, physiological, and immunological biomarkers. Fish Physiol. Biochem. **45**: 997–1013. doi:10.1007/s10695-019-00614-9

Aceves-Medina, G., E. A. González, and R. J. Saldierna. 1999. Larval development of Symphurus williamsi (Cynoglossidae: Pleuronectiformes) from the Gulf of California. Fish. Bull. **97**: 738–745.

Aceves-Medina, G., R. J. Saldierna-Martínez, and E. A. González. 2003. Distribution and abundance of Syacium ovale larvae (Pleuronectiformes: Paralichthyidae) in the Gulf of California. Rev. Biol. Trop. **51**: 561–567.

Archibald, K. M., D. A. Siegel, and S. C. Doney. 2019. Modeling the impact of zooplankton diel vertical migration on the carbon export flux of the biological pump. Global Biogeochem. Cycles **33**: 181–199. doi:10.1029/2018GB005983

Breitburg, D., and others. 2018. Declining oxygen in the global ocean and coastal waters. Science **1979**: 359. doi:10.1126/science.aam7240

Busecke, J. J. M., L. Resplandy, S. J. Ditkovsky, and J. G. John. 2022. Diverging fates of the Pacific Ocean oxygen minimum zone and its Core in a warming world. AGU Advances **3**: e2021AV000470. doi:10.1029/2021AV000470

Campbell, R. C., R. R. Sokal, and F. J. Rohlf. 1970. Biometry: The principles and practice of statistics in biological research. J. R. Stat. Soc. Ser. A **133**: 102. doi:10.2307/2343822

Cepeda-Morales, J., G. Gaxiola-Castro, E. Beier, and V. M. Godínez. 2013. The mechanisms involved in defining the northern boundary of the shallow oxygen minimum zone in the eastern tropical Pacific Ocean off Mexico. Deep Sea Res. Oceanogr. Res. Pap. **76**: 1–12. doi:10.1016/j.dsr.2013.02.004

Davies, S. M., L. Sánchez-Velasco, E. Beier, V. M. Godínez, E. D. Barton, and A. Tamayo. 2015. Three-dimensional distribution of larval fish habitats in the shallow oxygen minimum zone in the eastern tropical Pacific Ocean off Mexico. Deep Sea Res. Oceanogr. Res. Pap. **101**: 118–129. doi:10.1016/j.dsr.2015.04.003

Dixon, P. 2003. VEGAN, a package of R functions for community ecology. J. Veg. Sci. **14**: 927–930.

Espinoza-Morriberón, D., V. Echevin, D. Gutiérrez, J. Tam, M. Graco, J. Ledesma, and F. Colas. 2021. Evidences and drivers of ocean deoxygenation off Peru over recent past decades. Sci. Rep. **11**: 20292. doi:10.1038/s41598-021-99,876-8

Evseenko, S. A. 1990. Unusual larvae of the marine tonguefish, Symphurus sp.(Cynoglossidae), from central waters of the eastern Pacific. Vopr. Ikhtiol. **30**: 682–686.

Evseenko, S. A., and M. I. Shtaut. 2000. Early stages of development of two species of tongue soles–Symphurus chabanaudi and S. Prolatinaris (Cynoglossidae, Pleuronectiformes) from central eastern Pacific. J. Ichthyol. **40**: 751–761.

Fiedler, P. C., and L. D. Talley. 2006. Hydrography of the eastern tropical Pacific: A review. Prog. Oceanogr. **69**: 143–180. doi:10.1016/j.pocean.2006.03.008

Fiedler, P. C., and M. F. Lavín. 2017. Oceanographic Conditions of the Eastern Tropical Pacific. EPA, p. 59–83.

Froese, R., and D. Pauly. 2010. FishBase. WorldWideWeb Electronic Publication.

Gallo, N. D., and L. A. Levin. 2016. Fish ecology and evolution in the World's oxygen minimum zones and implications of ocean deoxygenation, p. 117–198. *In* Advances in marine biology. Academic Press.

Garcia, H. E., and others. 2019. World Ocean Atlas 2018, Volume 3: Dissolved oxygen, apparent oxygen utilization, and dissolved oxygen saturation. NOAA/NESDIS.

González-Navarro, E. A., R. J. Saldierna-Martínez, G. Aceves-Medina, and S. P. A. Jiménez-Rosenberg. 2013. Identification atlas of fish larvae of the Elopomorpha subdivision of the Mexican Pacific. CICIMAR Oceánides **28**: 7–40.

Gutiérrez-Bravo, J. G., L. Tenorio-Fernandez, S. P. A. Jiménez-Rosenberg, and L. Sánchez-Velasco. 2022. Three-dimensional distribution of larval fish habitats at the entrance of the Gulf of California in the tropical-subtropical convergence region off Mexico (April 2012). J. Plankton Res. **44**: 130–144. doi:10.1093/plankt/fbab085

Hjort, J. 1914. Fluctuations in the great fisheries of northern Europe viewed in the light of biological research. Conseil Permanent International pour l'exploration de la mer.

Houde, E. 1987. Fish early life dynamics and recruitment variability. Am. Fish. Soc. Symp. **2**: 17–29.

Houde, E. D. 2008. Emerging from Hjort's shadow. J. Northwest Atl. Fish. Sci. **41**: 53–70. doi:10.2960/J.v41.m634

Jiménez-Rosenberg, S. P. A., E. A. González-Navarro, and R. J. Saldierna-Martínez. 2006. Larval, prejuvenile and juvenile development of Eucinostomus currani. J. Fish Biol. **69**: 28–37.

Karstensen, J., L. Stramma, and M. Visbeck. 2007. Oxygen minimum zones in the eastern tropical Atlantic and Pacific oceans. Prog. Oceanogr. **77**: 331–350.

Koslow, J. A., R. Goericke, A. Lara-Lopez, and W. Watson. 2011. Impact of declining intermediate-water oxygen on deepwater fishes in the California current. Mar. Ecol. Prog. Ser. **436**: 207–218. doi:10.3354/meps09270

Kwiecinski, J. V., and A. R. Babbin. 2021. A high-resolution atlas of the eastern tropical Pacific oxygen deficient zones. Global Biogeochem. Cycles **35**: e2021GB007001. doi:10.1029/2021GB007001

Leon-Chávez, C. A., E. Beier, L. Sánchez-Velasco, E. D. Barton, and V. M. Godínez. 2015. Role of circulation scales and water mass distributions on larval fish habitats in the eastern tropical Pacific off Mexico. J. Geophys. Res. Oceans **120**: 3987–4002. doi:10.1002/2014JC010289

Maas, A. E., S. L. Frazar, D. M. Outram, B. A. Seibel, and K. F. Wishner. 2014. Fine-scale vertical distribution of macroplankton and micronekton in the eastern tropical North Pacific in association with an oxygen minimum zone. J. Plankton Res. **36**: 1557–1575. doi:10.1093/plankt/fbu077

Margolskee, A., H. Frenzel, S. Emerson, and C. Deutsch. 2019. Ventilation pathways for the North Pacific oxygen deficient zone. Global Biogeochem Cycles **33**: 875–890. doi:10.1029/2018GB006149

Moser, H. G. 1996. The early stages of fishes in the California Current region, Marine Life Research Program. Scripps Institution of Oceanography.

Nilsson, G. E., and S. Östlund-Nilsson. 2008. Does size matter for hypoxia tolerance in fish? Biol. Rev. **83**: 173–189. doi:10.1111/j.1469-185X.2008.00038.x

Olson, R. J., L. M. Duffy, P. M. Kuhnert, F. Galván-Magaña, N. Bocanegra-Castillo, and V. Alatorre-Ramírez. 2014. Decadal diet shift in yellowfin tuna Thunnus albacares suggests broad-scale food web changes in the eastern tropical Pacific Ocean. Mar. Ecol. Prog. Ser. **497**: 157–178. doi:10.3354/meps10609

Oschlies, A., O. Duteil, J. Getzlaff, W. Koeve, A. Landolfi, and S. Schmidtko. 2017. Patterns of deoxygenation: Sensitivity to natural and anthropogenic drivers. Philos. Trans. R. Soc. A Math. Phys. Eng. Sci. **375**: 20160325. doi:10.1098/rsta.2016.0325

Oschlies, A., P. Brandt, L. Stramma, and S. Schmidtko. 2018. Drivers and mechanisms of ocean deoxygenation. Nat. Geosci. **11**: 467–473. doi:10.1038/s41561-018-0152-2

Paulmier, A., and D. Ruiz-Pino. 2009. Oxygen minimum zones (OMZs) in the modern ocean. Prog. Oceanogr. **80**: 113–128. doi:10.1016/j.pocean.2008.08.001

Quintana-Rizzo, E., A. A. Cabrera, J. Ortiz-Wolford, and V. Dávila. 2021. Spatial distribution and abundance of small cetaceans in the Pacific waters of Guatemala. Front. Mar. Sci. **8**: 674134. doi:10.3389/fmars.2021.674134

Reygondeau, G., and others. 2018. Global biogeochemical provinces of the mesopelagic zone. J. Biogeogr. **45**: 500–514. doi:10.1111/jbi.13149

Richards, W. J. 2005. Early stages of Atlantic fishes: An identification guide for the western central north Atlantic, two volume set. CRC Press.

Robertson, D. R., and G. R. Allen. 2008. Shorefishes of the tropical eastern Pacific. Smithsonian Tropical Research Institute.

Sánchez-Velasco, L., V. M. Godínez, E. D. Ruvalcaba-Aroche, A. Márquez-Artavia, E. Beier, E. D. Barton, and S. P. A. Jiménez-Rosenberg. 2019. Larval fish habitats and deoxygenation in the northern limit of the oxygen minimum zone off Mexico. J. Geophys. Res. Oceans **124**: 9690–9705. doi:10.1029/2019JC015414

Sánchez-Velasco, L., and others. 2022. Vertical distribution of zooplankton groups, with an emphasis on fish larvae, in the oxygen minimum zone off southern México (December 2020). J. Mar. Syst. **236**: 103801. doi:10.1016/j.jmarsys.2022.103801

Siegel, D. A., T. Devries, I. C. Cetini´c, and K. M. Bisson. 2023. Quantifying the Ocean's biological pump and its carbon cycle impacts on global scales. Ann. Rev. Mar. Sci. **15**: 329–356. doi:10.1146/annurev-marine-040722

Silva-Segundo, C. A., R. Funes-Rodríguez, J. Gómez-Gutiérrez, G. Gallegos-Simental, S. Hernández-Trujillo, and A. Blanco-Jarvio. 2021. DNA barcoding and taxonomic validation of Caranx spp. larvae. J. Mar. Biol. Assoc. UK **101**: 399–407.

Sokal, R., and F. Rohlf. 1995. Biometry, 3rd ed. Freeman.

Steedman, H. F. 1976. Zooplankton fixation and preservation. Unesco Press.

Stewart, J. D., A. Barroso, R. H. Butler, and R. J. Munns. 2018. Caught at the surface. Ecology **99**: 1894–1896. doi:10.2307/26626157

Stramma, L., G. C. Johnson, J. Sprintall, and V. Mohrholz. 2008. Expanding oxygen-minimum zones in the tropical oceans. Science **1979**: 655–658. doi:10.1126/science.1151751

Stramma, L., and others. 2012. Expansion of oxygen minimum zones may reduce available habitat for tropical pelagic fishes. Nat. Clim. Chang. **2**: 33–37. doi:10.1038/nclimate1304

Sutton, T. T., P. H. Wiebe, L. Madin, and A. Bucklin. 2010. Diversity and community structure of pelagic fishes to 5000 m depth in the Sargasso Sea. Deep Sea Res. Top. Stud. Oceanogr. **57**: 2220–2233. doi:10.1016/j.dsr2.2010.09.024

Sutton, T. T., and others. 2017. A global biogeographic classification of the mesopelagic zone. Deep Sea Res. Oceanogr. Res. Pap. **126**: 85–102. doi:10.1016/j.dsr.2017.05.006

Ter Braak, C. J. F. 1986. Canonical correspondence analysis: A new eigenvector technique for multivariate direct gradient analysis. Ecology **67**: 1167–1179.

Tiano, L., E. Garcia-Robledo, T. Dalsgaard, A. H. Devol, B. B. Ward, O. Ulloa, D. E. Canfield, and N. Peter Revsbech. 2014. Oxygen distribution and aerobic respiration in the north and south eastern tropical Pacific oxygen minimum zones. Deep Sea Res. Oceanogr. Res. Pap. **94**: 173–183. doi:10.1016/j.dsr.2014.10.001

Villarroel del Pino, L. A. 2018. Test de hipótesis y asociación de variables, p. 135–206. *In* Métodos Bioestadísticos. Ediciones UC.

Voesenek, C. J., F. T. Muijres, and J. L. Van Leeuwen. 2018. Biomechanics of swimming in developing larval fish. J. Exp. Biol. **221**: jeb149583. doi:10.1242/jeb.149583

Walsh, W. A., C. Swanson, C.-S. Lee, J. E. Banno, and H. Eda. 1989. Oxygen consumption by eggs and larvae of striped mullet, Mugil cephalus, in relation to development, salinity and temperature. J. Fish. Biol. **35**: 347–358. doi:10.1111/j.1095-8649.1989.tb02987.x

Wiebe, P. H., A. W. Morton, A. M. Bradley, R. H. Backus, E. Craddock, V. Barber, T. J. Cowles, and G. R. Flierl. 1985. New developments in the MOCNESS, an apparatus for sampling zooplankton and micronekton. Mar. Biol. **87**: 313–323.

Wiebe, P. H., D. Allison, M. Kennedy, and G. Moncoiffé. 2015. A vocabulary for the configuration of net tows for collecting plankton and micronekton. J. Plankton Res. **37**: 21–27. doi:10.1093/plankt/fbu101

Wishner, K. F., D. M. Outram, B. A. Seibel, K. L. Daly, and R. L. Williams. 2013. Zooplankton in the eastern tropical north Pacific: Boundary effects of oxygen minimum zone expansion. Deep Sea Res. Oceanogr. Res. Pap. **79**: 122–140. doi:10.1016/j.dsr.2013.05.012

Wishner, K. F., and others. 2018. Ocean deoxygenation and zooplankton: Very small oxygen differences matter. Sci. Adv. **4**: 5180.

Acknowledgments

We would like to thank the crew of the *RV Sally Ride* for their help during fieldwork. We would also like to thank the Ichthyoplankton laboratory of CICIMAR for their help with fish larvae ID. J.G.G.B. would like to thank CONAHCyT for his research assistantship. L.S.V. would like to thank Instituto Politécnico Nacional for support during a sabbatical semester. This research was funded by the National Science Foundation Division of Ocean Sciences Grant # 1851361.

Conflict of Interest

None declared.

Submitted 20 October 2023
Revised 29 February 2024
Accepted 12 May 2024

Associate editor: Kelly J. Benoit-Bird